*J. Mater. Environ. Sci. 7 (3) (2016) 878-888*
*ISSN : 2028-2508*
*CODEN: JMESCN*



# Anti-corrosive properties of new Benzothiazine derivative on mild steel corrosion in 1 M HCl: Experimental and theoretical investigations

**M. Boudalia[1*], N.K. Sebbar [2], H. Bourazmi [1], S. Lahmidi [2], Y. Ouzidan [3], E.M. Essassi [2], H. Tayebi[1], A. Bellaouchou[1], A. Guenbour[1], A. Zarrouk[4]**

[1]*Laboratoire de Nanotechnologie,Matériaux et environnement- Faculté des Sciences, Université Mohamed V, Av. Ibn Batouta, BP. 1014 Rabat, Morocco*
[2]*Laboratoire de Chimie Organique Hétérocyclique, URAC 21, Pôle de Compétences Pharmacochimie, Université Mohammed V, Faculté des Sciences, Av. Ibn Battouta, BP 1014 Rabat, Morocco.*
[3]*Laboratoire de Chimie Organique Appliquée, Faculte des Sciences et Techniques, Universite´ Sidi Mohamed Ben Abdallah, Fes, Maroc.*
[4] *LCAE-URAC18, Faculty of Science, Mohammed first University, Po Box 717, 60000 Oujda, Morocco.*

*Received 22May 2015, Revised 21 Sep 2015, Accepted 23 Sep 2015*
[*]*Corresponding author: E-mail: maria.boudalia@yahoo.fr*

## Abstract

The effect of adding [(E)-2-benzylidene-4-(prop-2-ynyl)-2H-benzo[b][1,4]thiazin-3(4H)-one] named (P1), newly synthesized on the electrochemical behavior of mild steel in molar hydrochloric acid was investigated by using the potentiodynamic polarization and electrochemical impedance spectroscopy (EIS) measurements. EIS diagrams show that adsorption of (P1) increases the transfer resistance and decrease the capacitance of interface metal/solution. The inhibition efficiency for this compound studied increased with the increase in the inhibitor concentrations to attain 94% at the $10^{-4}$ M of (P1). The inhibitor (P1) was adsorbed on the steel surface according to the Langmuir adsorption isotherm model. From the adsorption isotherm, some thermodynamic data for the adsorption process were calculated and discussed. Kinetic parameters activation such as activation energy, entropy and enthalpy of activation were evaluated from the effect of temperature on corrosion and inhibition processes. Correlation between quantum chemical calculations and inhibition efficiency of the investigated compound is discussed using the Density Functional Theory method (DFT).

*Key words*:leets dliM, lCH, Corossion, inhibition, Langmuir, EIS, Benzothiazine derivative. DFT.

## I. Introduction:

Organic compounds containing polar groups by which the molecule can become strongly or specifically adsorbed on the metal surface constitute most organic inhibitors [1,2].
These inhibitors, which include the organic N, P, S, and OH groups, are known to be similar to catalytic poisons as they decrease the reaction rate at metal/solution interface without in general, being involved in the reaction considered. It is generally accepted that most organic inhibitors act via adsorption at the metal/solution interface. The mechanism by which an inhibitor decreases the corrosion current is achieved by interfering with some of the steps for the electrochemical process. The corrosion inhibition of mild steel in aggressive acidic solutions has been widely investigated.
In industries, hydrochloric acid solutions are often used in order to remove scale and salts from steel surfaces, and cleaning tanks and pipelines. This treatment may be prerequisite for coating by electroplating, galvanizing, or painting techniques. The acid must be treated to prevent an extensive dissolution of the underlying metal. This treatment involves the addition of some organic inhibitors to the acid solution that adsorb at the metal/solution interface by displacing water molecules on the surface and forming a compact barrier film. The choice of the inhibitor is based on two considerations, first economic consideration and second, should contain the electron cloud on the aromatic ring or the electronegative atoms such as N, O in the relatively long chain compounds. Generally the organic compounds containing hetero atoms like O, N, S, and P are found to work as very effective corrosion

inhibitors. The efficiency of these compounds depends upon electron density present around the hetero atoms, the number of adsorption active centers in the molecule and their charge density, molecular size, mode of adsorption, and formation of metallic complexes [3-31]. These compounds in general are adsorbed on the metal surface, blocking the active corrosion sites. Four types of adsorption may take place by organic molecules at metal/solution interface:
(a) electrostatic attraction between the charged molecules and the charged metal
(b) interaction of unshared electron pairs in the molecule with the metal
(c) interaction of π-electrons with the metal
(d) combination of a and c
The adsorption ability of inhibitors onto metal surface depends on the nature and surface charge of metal, the chemical composition of electrolytes, and the molecular structure and electronic characteristics of inhibitor molecules.
Density functional theory (DFT) has grown to be a useful theoretical method to interpret experimental results, enabling one to obtain structural parameters for even huge complex molecules, and it can explains the hard and soft acid base (HSAB) behavior of organic molecules, i.e., DFT connects some traditional empirical concepts with quantum mechanical interpretations [32,33]. Therefore, DFT is a very powerful technique to probe the inhibitor/surface interaction and to analyze experimental data. The aim of the present work is to investigate the effects of (E)-2-benzylidene-4-(prop-2-ynyl)-2H-benzo[b][1,4]thiazin-3(4H)-one (P1) as corrosion inhibitor for mild steel in 1 M HCl solution using electrochemical techniques. Thermodynamic activation parameters were evaluated from experimental data. The relationships between the inhibition performances of the investigated inhibitor in 1 M HCl and some quantum chemical parameters, such as the highest occupied molecular orbital energy ($E_{HOMO}$), the lowest unoccupied molecular orbital energy ($E_{LUMO}$), the energy gap between $E_{LUMO}$ and $E_{HOMO}$ ($\Delta E_{LUMO-HOMO}$) and dipole moments. The molecular structure of P1 is given in scheme 1.

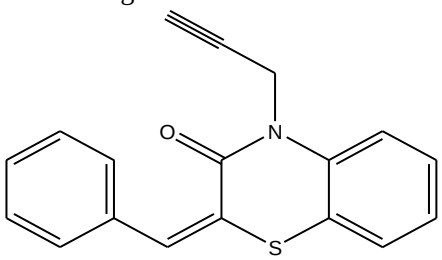


**Scheme 1:** (E)-2-benzylidene-4-(prop-2-ynyl)-2H-benzo[b][1,4]thiazin-3(4H)-one (P1).

## 2. Experimental details

2.1. Materials and solutions

Mild steel was used for this study has the following composition: (0.37% C, 0.23%Si, 0.016 S%, 0,68 Mn%, 0.16 Cu%, 0.077Cr%, 0.011Ti%, 0,052Ni%, 0.009 Co% ) and Fe
The aggressive solutions of 1.0 M HCl were prepared by dilution of analytical grade 37% HCl with distilled water. The concentration range of E)-2-benzylidene-4-(prop-2-ynyl)-2H-benzo[b][1,4]thiazin-3(4H)-one (P1) used was $10^{-7}$M to $10^{-4}$M.

2.2. Synthesis of inhibitor

To a mixture of (2Z)-2-(benzylidene)-3,4-dihydro-2H-1,4-benzothiazin-3-one (0.38 g, 1.5 mmol), potassium carbonate (0.24 g, 1.8 mmol) and tetra n-butyl ammonium bromide (0.05 g, 0.15 mmol) in DMF (25 ml) was added propargyl bromide (0.12 ml, 1.6 mmol). Stirring was continued at room temperature for 24 h. The salt was removed by filtration and the filtrate was concentrated under reduced pressure. The residue was separated by chromatography on a column of silica gel with ethyl acetate-hexane (1:2) as eluent; yellow crystals were obtained upon evaporation of the solvent (yield = 55%) (scheme 2).

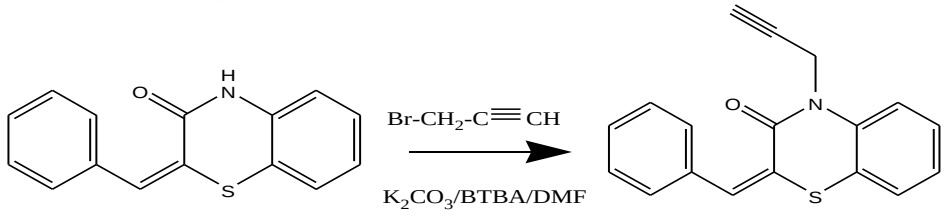


**Scheme 2:** Characterization of (E)-2-benzylidene-4-(prop-2-ynyl)-2H-benzo[b][1,4]thiazin-3(4H)-one
Yield = 55%; F (°C) = 130-132.

RMN$^{1}$H (DMSO-$d_6$) δ ppm : 2.48(t, 1H, -C≡CH, J=1,8Hz); 4.85 (d, 2H, $NCH_2$, J=2,4Hz); 7.84(s, 1H; =CH); 7.09-7.66 (m, 9H, $H_{ar}$). RMN$^{13}$C (DMSO-$d_6$) δ ppm : 34.9 ($NCH_2$); 75.4 (-C≡CH); 126.8 (=CH); 117.8, 118.3, 124.4, 126.8, 2* 128.1, 129.1, 2*129.7, 130.6 ($CH_{ar}$) ; 79.6, 134.4, 2*135.4, 135.8 (Cq), 165.1 (C=O).

2.3. Electrochemical measurements

The electrochemical measurements were carried out using a Volta lab (Tacussel- Radiometer PGZ 100) potentiostate and controlled by Tacussel corrosion analysis software model (Voltamaster 4) at under static condition. The corrosion cell used had three electrodes. The reference electrode was a saturated calomel electrode (SCE). A platinum electrode was used as auxiliary electrode of surface area of 1 $cm^2$. The working electrode was carbon steel with the surface area of 1 $cm^2$. All potentials given in this study were referred to this reference electrode. The working electrode was immersed in test solution for 30 minutes to a establish steady state open circuit potential (Eocp). After measuring the Eocp, the electrochemical measurements were performed. All electrochemical tests have been performed in aerated solutions at 303 K. The EIS experiments were conducted in the frequency range with high limit of 100 kHz and different low limit 0.1 Hz at open circuit potential, with 10 points per decade, at the rest potential, after 30 min of acid immersion, by applying 10 mV ac voltage peak-to-peak. Nyquist plots were made from these experiments. The best semicircle can be fit through the data points in the Nyquist plot using a non-linear least square fit so as to give the intersections with the x-axis.

The inhibition efficiency of the inhibitor was calculated from the charge transfer resistance values using the following equation:

$$\eta_z\,\% = \frac{R_{ct}^{i} - R_{ct}^{\circ}}{R_{ct}^{i}} \times 100 \qquad (1)$$

Where, $R_{ct}^{\circ}$ and $R_{ct}^{i}$ are the charge transfer resistance in absence and in presence of inhibitor, respectively.

After ac impedance test, the potentiodynamic polarization measurements of mild steel substrate in inhibited and uninhibited solution were scanned from cathodic to the anodic direction, with a scan rate of 2 mV $s^{-1}$. The potentiodynamic data were analysed using the polarization VoltaMaster 4 software. The linear Tafel segments of anodic and cathodic curves were extrapolated to corrosion potential to obtain corrosion current densities ($I_{corr}$). The inhibition efficiency was evaluated from the measured $I_{corr}$ values using the following relationship:

$$\eta_{Tafel}\,\% = \frac{I_{corr}^{\circ} - I_{corr}^{i}}{I_{corr}^{\circ}} \times 100 \qquad (2)$$

where $I_{corr}$ and $I_{corr(i)}$ are the corrosion current densities for steel electrode in the uninhibited and inhibited solutions, respectively.

2.4. Quantum chemical calculations

Density Functional theory (DFT) has been recently used [34-37], to describe the interaction between the inhibitor molecule and the surface as well as the properties of these inhibitors concerning their reactivity. The molecular band gap was computed as the first vertical electronic excitation energy from the ground state using the time-dependent density functional theory (TD-DFT) approach as implemented in Gaussian 03[38]. For these seek, some molecular descriptors, such as HOMO and LUMO energy values, frontier orbital energy gap and molecular dipole moment, were calculated using the DFT method and have been used to understand the properties and activity of the newly prepared compounds and to help in the explanation of the experimental data obtained for the corrosion process.

## 3. Results and discussion

3.1. Polarization study:

The kinetics of the cathodic and anodic reactions occurring on working electrode in 1 M HCl in the absence and presence of P1 were studied through the potentiodynamic polarization measurements and the polarization curves are shown in Fig. 1. The values of related electrochemical parameters, i.e., corrosion potential ($E_{corr}$), corrosion current density ($I_{corr}$), and Tafel slopes ($\beta_c$ and $\beta_a$), obtained by extrapolating the anodic and cathodic Tafel curves are listed in Table 1. It can be seen that the addition of P1 causes a remarkable shift in both anodic and cathodic Tafel curves to lower current densities (Fig. 1). This phenomenon indicates that both anodic metal dissolution and cathodic hydrogen evolution reactions are drastically inhibited. The cathodic Tafel curves give rise to almost parallel lines, meaning the

hydrogen evolution is activation-controlled and the reduction of $H^+$ on the working electrode surface occurs mainly through a charge transfer mechanism [39]. For the anodic part of the Tafel curves, it is apparent that the anodic reaction is evidently inhibited in the presence of P1. The higher concentration of P1 provides better inhibition efficiency.

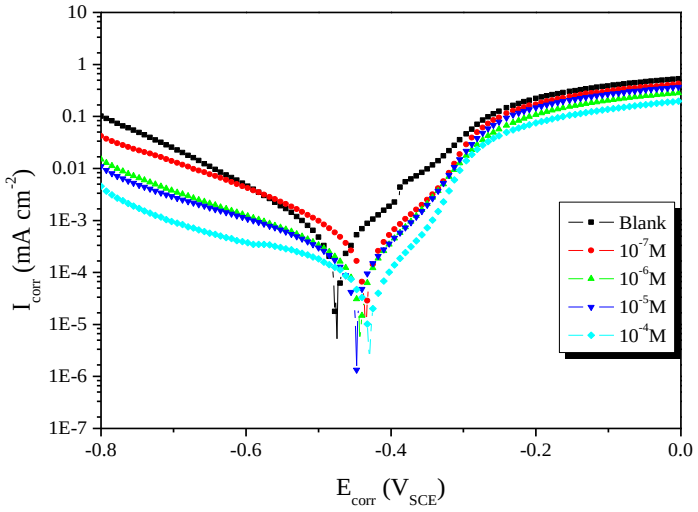


**Figure 1:** Polarization curves of mild steel in 1M HCl containing different concentrations of P1.

**Table 1:** Polarization parameters and the corresponding inhibition efficiency for the corrosion of mild steel in 1 M HCl containing different concentrations of P1 at 303K.

| Inhibitor | Conc (M) | $-E_{corr}$ ($mV_{SCE}$) | $\beta_a$ (mV/dec) | $-\beta_c$ (mV/dec) | $I_{corr}$ ($\mu A\ cm^{-2}$) | $\eta_{Tafel}$ (%) |
|---|---|---|---|---|---|---|
| Blank | — | 477 | 101 | 138 | 579 | — |
| P1 | $10^{-7}$ | 439 | 96.4 | 128 | 130 | 78 |
| | $10^{-6}$ | 444 | 77.2 | 132 | 85 | 85 |
| | $10^{-5}$ | 449 | 95.0 | 177 | 75 | 87 |
| | $10^{-4}$ | 432 | 93.0 | 211 | 40 | 93 |

With the inspection of Table 1, we found that there is no obvious shift in the corrosion potential in response to addition of different P1 concentrations, which can be interpreted that P1 acts as a mixed type inhibitor. After addition of P1 to the blank solution, the values of corrosion current density decrease, and the inhibition efficiencies increase density decrease, and the inhibition efficiencies increase sharply. As can be seen from Table 1, $E_{corr}$ values are slightly changed (only the displacement was $\leq$ 45 mV) [40,41], in the presence of P1 with respect to blank suggesting that the P1 acts as mixed type inhibitor.

*3.2. Electrochemical impedance spectroscopy measurements*

The corrosion behavior of mild steel, in acidic solution containing different concentration of benzothiazine derivative (P1) compound, was investigated by the EIS at 303K after 30 min of immersion. The obtained results are presented in Figure 2. The impedance parameters calculated are given in Table 2.

The curves show a similar type of Nyquist plot for mild steel in the presence of various concentrations of P1. The simple equivalent Randle circuit for studies was shown in figure 3, where $R_\Omega$ represents the solution and corrosion product film resistance, the parallel combination of resister, $R_{ct}$ and capacitor $C_{dl}$ represents the corroding interface. The existence of single semi circle showed the single charge transfer process during dissolution which is unaffected by the presence of inhibitor molecules. Deviations of perfect circular shape are often refereed to the frequency dispersion of interfacial impedance which arises due to the roughness and other inhomogeneity of the surface [42, 43]. As seen from Table 2, the $R_{ct}$ values of inhibited substrates are increased with the concentration of inhibitors. On the other hand, the values of $C_{dl}$ are decreased with increase in inhibitor concentration which is most probably is due to the decrease in local dielectric constant and / or increase in thickness of the electrical double layer, suggests that P1 act via adsorption at the metal / solution interface [44,45].

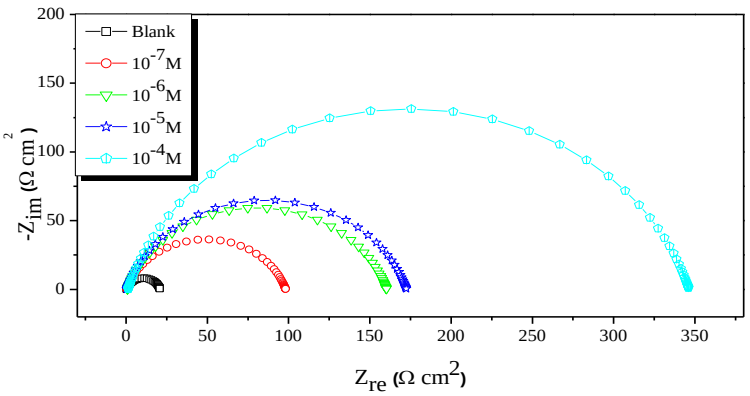


**Figure 2:** Nyquist plots of mild steel in 1M HCl without and with different concentrations of (P1) at 303K.

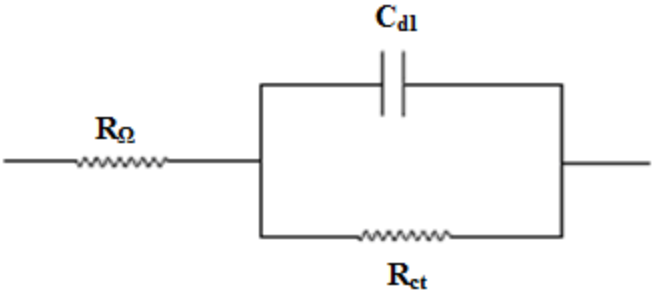


**Figure 3:** The electrochemical equivalent circuit used to fit the impedance measurements.

**Table 2:** Impedance parameters of mild steel in 1M HCl containing different concentrations of P1 at 303K.

| Inhibitor | Conc (M) | $R_{ct}$ ($\Omega$ cm$^2$) | $f_{max}$ (Hz) | $C_{dl}$ ($\mu$F/cm$^2$) | $\eta_z$ (%) |
|---|---|---|---|---|---|
| Blank | 1.0 | 20 | 63 | 126 | --- |
| P1 | $10^{-7}$ | 99 | 20 | 80 | 80 |
| | $10^{-6}$ | 164 | 16 | 61 | 88 |
| | $10^{-5}$ | 176 | 20 | 45 | 89 |
| | $10^{-4}$ | 359 | 20 | 22 | 94 |

3.3. Kinetic-thermodynamic corrosion parameters

To evaluate the adsorption of P1 and activation parameters of the corrosion processes of mild steel in acidic media, polarization measurements are investigated in the absence and presence of inhibitor and also in the range of temperature 303-333 K. The numerical values of the variation of corrosion current density ($I_{corr}$), corrosion potential ($E_{corr}$), anodic and cathodic Tafel slopes at all studied temperatures are given in Table 3.

Close examination of Table 3 shows that an increase in temperature increases $I_{corr}$, while the addition of P1 decreases the $I_{corr}$ values across the temperature range. The results also indicate that the inhibition efficiencies increased with the concentration of inhibitor but decreased proportionally with temperature. Such behavior can be interpreted on the basis that the inhibitor acts by adsorbing onto the metal surface, and an increase in temperature results in the desorption of some adsorbed inhibitor molecules, leading to a decrease in the inhibition efficiency [46].

The activation parameters for the corrosion process were calculated from Arrhenius-type plot according to the following equation:

$$I_{corr} = k \exp\left(\frac{-E_a}{RT}\right) \quad (3)$$

where $E_a$ is the apparent activation corrosion energy, R is the universal gas constant and k is the Arrhenius pre-exponential constant.

**Table 3:** Polarisation parameters for M steel in 1M HCl with optimum concentration of P1 at different temperatures

| T (K) | Inh | $-E_{corr}$ ($mV_{SCE}$) | $\beta_a$ ($mV\ dec^{-1}$) | $-\beta_c$ ($mV\ dec^{-1}$) | $I_{corr}$ ($\mu A\ cm^{-2}$) | $\eta_{Tafel}$ (%) |
|---|---|---|---|---|---|---|
| 303 | Blank | 477 | 101 | 138 | 579 | — |
| | $10^{-4}$M | 432 | 93 | 211 | 40 | 93 |
| 313 | Blank | 448 | 43 | 57 | 781 | — |
| | $10^{-4}$M | 481 | 99 | 93 | 130 | 83 |
| 323 | Blank | 457 | 106 | 107 | 882 | — |
| | $10^{-4}$M | 488 | 81 | 102 | 211 | 77 |
| 333 | Blank | 475 | 60 | 161 | 999 | — |
| | $10^{-4}$M | 491 | 128 | 129 | 298 | 70 |

Arrhenius plots for the corrosion density of mild steel in the case of P1 are given in Fig.4. Values of apparent activation energy of corrosion ($E_a$) for mild steel in 1 M HCl with the absence and presence of P1 at optimum concentration were determined from the slope of Ln ($I_{corr}$) versus 1/T plots and shown in Table 4.

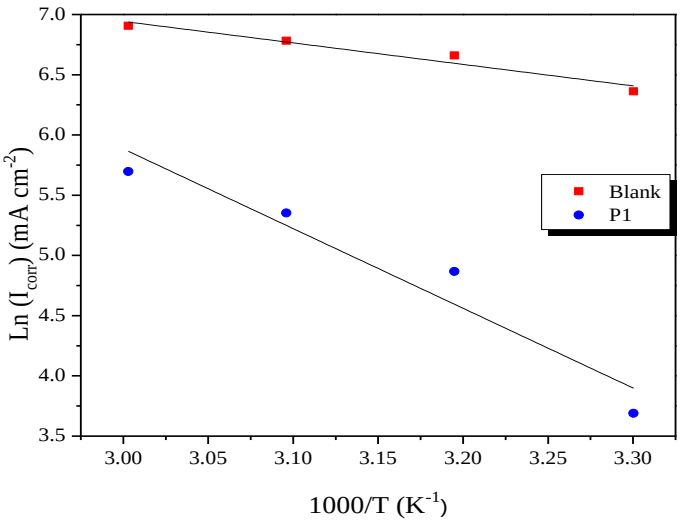


**Figure 4:** Arrhenius plots of mild steel in 1 M HCl with and without $10^{-4}$ M of P1.

From table 4, the activation energy for the corrosion process increases from 14.83 to 55.01 kJ $mol^{-1}$. The increase in the corrosion current density and the activation energy indicate that dissolution of mild steel in 1 M HCl in the presence of inhibitor is lower than in the solution with no inhibitor. It has been reported that higher $E_a$ in the presence of inhibitor for carbon steel in comparison with blank solution is typically indicative of physisorption [47].
An alternative formulation of Arrhenius equation is:

$$I_{corr} = \frac{RT}{Nh} \exp\left(\frac{\Delta S_a}{R}\right) \exp\left(\frac{\Delta H_a}{RT}\right) \quad (4)$$

where $I_{corr}$ is the corrosion rate, A is the pre-exponential factor, h is Planck's constant, N is the Avogadro number, R is the universal gas constant, $\Delta H_a$ is the enthalpy of activation and $\Delta S_a$ is the entropy of activation.

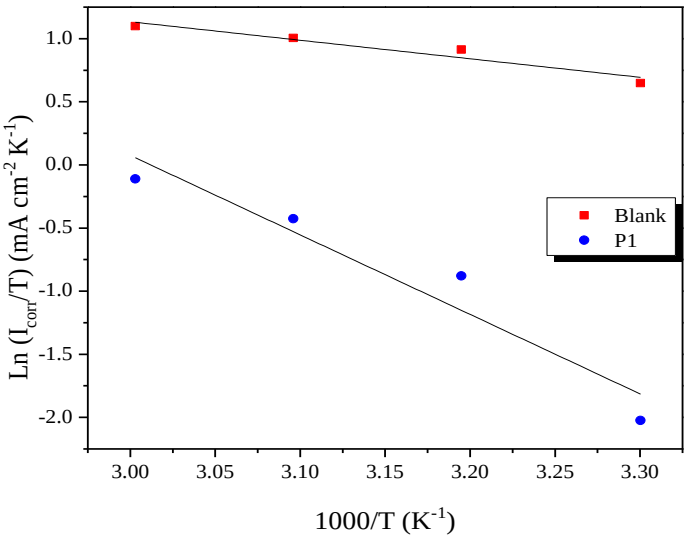


**Figure 5:** Transition arrhenius plots of Ln ($I_{corr}$) versus 1000/T with and without optimum concentration of P1.

**Table 4:** The values of activation parameters $E_a$, $\Delta H_a$ and $\Delta S_a$ for mild steel in 1 M HCl in the absence and presence of $10^{-4}$ M of P1.

| Medium | $E_a$ (kJ/mol) | $\Delta H_a$ (kJ/mol) | $\Delta S_a$ (J $mol^{-1}$ $K^{-1}$) |
|---|---|---|---|
| Blank | 14.83 | 12.19 | -151.54 |
| P1 | 55.01 | 52.37 | -39.79 |

Fig. 5 shows a plot of Ln ($I_{corr}$/T) against 1/T. Straight lines are obtained with a slope of ($-\Delta H_a$ /R) and an intercept of (Ln(R/Nh) + ($\Delta S_a$/R)) from which the values of $\Delta H_a$ and $\Delta S_a$ are calculated and listed in Table 4. The analysis of the results of Table 4 shows that the activation energy $E_a$ and activation heat $\Delta H_a$ against the P1 vary in the same manner. The thermodynamic parameters ($\Delta H_a$ and $\Delta S_a$) of the dissolution reaction of steel in 1 M HCl in the presence of P1 is higher than that of in the absence of inhibitor (blank). The positive signs of the enthalpies $\Delta H_a$ reflect the endothermic nature of the steel dissolution process and mean that the dissolution of steel is difficult [48]. In the presence of P1, the increase of $\Delta S_a$ reveals that an increase in disordering takes place on going from reactants to the activated complex [49].

3.4. Adsorption isotherm and thermodynamic parameters

It is well recognized that the first step in inhibition of metallic corrosion is the adsorption of organic inhibitor molecules at the metal/solution interface and that the adsorption depends on the molecules chemical composition, the temperature and the electrochemical potential at the metal/solution interface. In fact, the solvent $H_2O$ molecules could also adsorb at metal/solution interface. So the adsorption of organic inhibitor molecules from the aqueous solution can be regarded as a quasi-substitution process between the organic compounds in the aqueous phase [Org(sol)] and water molecules at the electrode surface [$H_2O$ (ads)] [50]:

Org (sol) + $nH_2O$ (ads) ↔ Org (ads) + $nH_2O$ (sol)

Where (n) is the size ratio, that is, the number of water molecules replaced by one organic inhibitor. Basic information on the interaction between they inhibitor and the steel surface can be provided by the adsorption isotherm. In order to obtain the isotherm, the linear relation between degree of surface coverage (θ) values ($\theta$=$\eta_{Tafel}$%/100) and inhibitor concentration (C) must be found. Attempts were made to fit the θ values to various isotherms including Langmuir, Temkin and Frumkin. By far the best fit is obtained with the Langmuir isotherm. This model has also been used for other inhibitor systems [51, 52]. According to this isotherm, θ is related to C by:

Langmuir: $\frac{C}{\theta} = \frac{1}{k} + C$ (5)

Frumkin :$\mathrm{Ln}\left(\mathrm{C}\left(\frac{1-\theta}{\theta}\right)\right) = LnK + g\theta$ (6)

Temkin : $Ln\left(\frac{\theta}{C}\right) = LnK - g\theta$ (7)

The θ is the surface coverage, K is the adsorption-desorption equilibrium constant, C is the concentration of inhibitor and is the adsorbate parameter.

Figure 6 shows the plots of C/θ versus C and the expected linear relationship is obtained for this compound. The strong correlation ($R^2$ = 0.99994 for the compound P1) confirm the validity of this approach. The thermodynamic parameters from the Langmuir adsorption isotherm are listed in Table 5, together with the value of the Gibbs free energy of adsorption $\Delta G^{\circ}_{ads}$ calculated from the equation

$$\Delta G^{\circ}_{ads} = -RTLn(55.5K_{ads}) \quad (8)$$

where R is the universal gas constant, T is the absolute temperature and the value of 55.5 is the concentration of water in the solution [53].

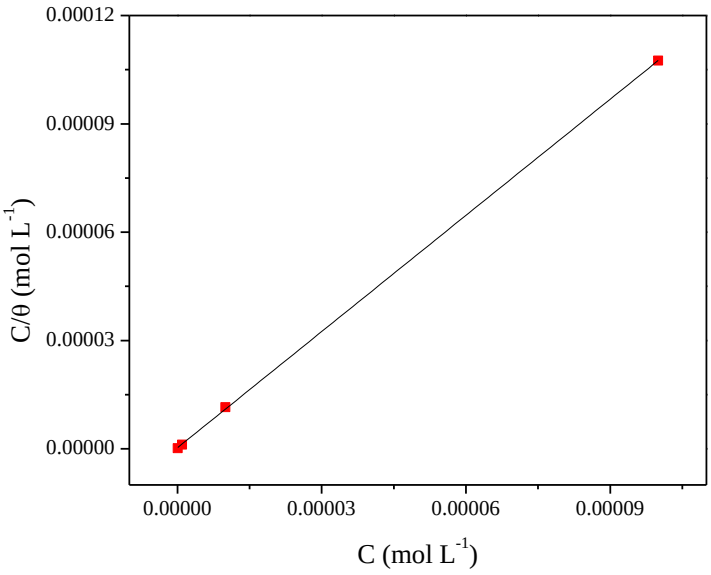


**Figure 6:** Langmuir isotherm adsorption model of P1 on the surface of mild steel in 1M HCl.

The parameters calculated from the Langmuir adsorption isotherm model are reported in Table 5.

**Table 5:** Langmuir adsorption parameters.

| Medium | Slope | $K_{ads}$ ($M^{-1}$) | $R^2$ | $\Delta G^{\circ}_{ads}$ (kJ/mol) |
|---|---|---|---|---|
| P1 | 1.07 | 3558174.37 | 0.99994 | -48.11 |

From table 5, the negative values of standard free energy of adsorption indicate spontaneous adsorption of organic molecules on metallic surface and also the strong interaction between inhibitor molecules and mild steel surface [54,55]. Generally, the standard free energy values of - 20 kJ $mol^{-1}$ or less negative are associated with an electrostatic interaction between charged molecules and charged metal surface (physical adsorption); those of - 40 kJ $mol^{-1}$ or more negative involves charge sharing or transfer from the inhibitor molecules to the metal surface to form a co-ordinate covalent bond (chemical adsorption) [56,57]. Based on the literature [58], the calculated $\Delta G^{\circ}_{ads}$ value in this work indicates that the adsorption mechanism of P1 on mild steel is chemisorption.

### *3.5. Quantum chemical calculations*

In order to investigate the correlation between the molecular structure of the inhibitor and its inhibition effect, quantum chemical calculations have been performed. Fig. 7 shows the optimized geometric structure and the electron density distribution of both HOMO and LUMO. The related quantum chemical parameters including $E_{HOMO}$, $E_{LUMO}$, ΔE and μ are given in Table 6. From Fig. 7, it can be found that the electron density distribution of HOMO is localized on the whole molecule, whereas the LUMO density is mainly located on a benzene ring and the hetero atoms.

**(a)**

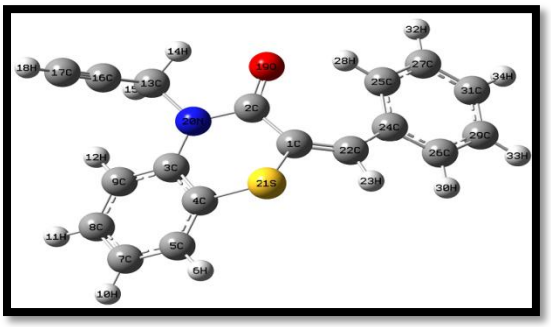

**(b)** **(c)**

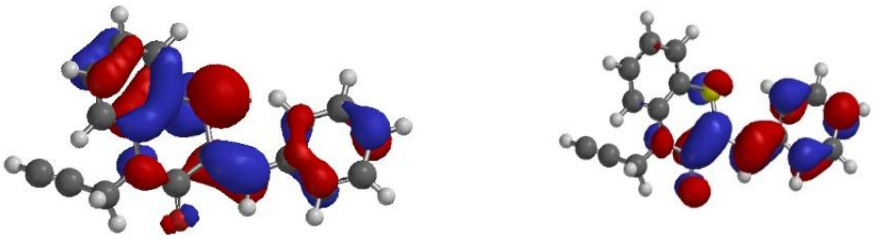

**Figure 7:** Optimized geometric structure (a) and the electron density distributions of both HOMO (b) and LUMO (c) for the P1.

It is well known that HOMO is often associated with the ability of the molecule to donate electron and high $E_{HOMO}$ value means a strong electron-donating ability [59-63], while LUMO indicates the electron-accepting ability of the molecule and the lower value of $E_{LUMO}$ indicates that the molecule would more probably accept electrons [59-63]. The energy gap (ΔE) between HOMO and LUMO reflects the stability of the molecule, a smaller ΔE implies that the molecule is much easier to be polarized and adsorbed on the metal surface [59,62-64]. In addition, owing to the dipole-dipole interaction between molecules and metal surface, high values of the dipole moment can lead to stronger inhibition [62,63]. The results of Table 6 shows that the values of $E_{HOMO}$ and $E_{LUMO}$ are lower, which indicates the P1 cation is more likely to accept electrons rather than donate electrons. The μ of the P1 cation is higher than that of $H_2O$ [62]. The high value of μ probably increases the adsorption between the P1 cation and metal surface [62].

**Table 6:** The computed molecular parameters for P1 compound.

| $E_{HOMO}$ (eV) | $E_{LUMO}$ (eV) | $\Delta E$ gap (eV) | $\mu$ (debye) |
|---|---|---|---|
| -6.367 | -1.741 | 4.626 | 2.9246 |

## Conclusion:

The main conclusions drawn from this study are:

1. of (E)-2-benzylidene-4-(prop-2-ynyl)-2H-benzo[b][1,4]thiazin-3(4H)-one (P1) inhibits the corrosion of mild steel in 1M HCl.
2. The inhibition efficiency increases with increasing inhibitor concentrations to attain a maximum value of 94 % for inhibitor P1 at $10^{-4}$ M,
3. The inhibition efficiency decreased with increasing temperature as a result of the higher dissolution of steel at higher temperature.

4. P1 acted through adsorption on the mild steel surface and its adsorption obeyed the Langmuir adsorption isotherm.
5. Potentiodynamic polarization curve reveals that P1 belonged to mixed-type inhibitor.
6. Impedance method indicates that Benzothiazine derivative adsorbs on mild steel surface with increasing charge-transfer resistance and decreasing the double-layer capacitance,
7. Comparison between the theoretical findings satisfactorily correlates with experimental results and validate the method employed here.

**References:**

1. Damaskin B. B., Pietrij O. A., Batrokov W.W., *Moskva*. (1968).
2. Okamoto G., Nagayama M., Kato J., Baba T., *Corros Sci*. 2 (1996) 27.
3. Beloglazov S. M., Dzhafarov Z. I., Polyakov V. N., Demushia N.N., *Prot. Met*. 27 (1991) 813.
4. Al Hamzi A.H., Zarrok H., Zarrouk A., Salghi R., Hammouti B., Al-Deyab S.S., Bouachrine M., Amine A., Guenoun F., *Int. J. Electrochem*. Sci. 8 (2013) 2586.
5. Zarrouk A., Hammouti B., Zarrok H., Warad I., Bouachrine M., *Der Pharm. Chem*. 3 (2011) 263.
6. Ben Hmamou D., Salghi R., Zarrouk A., Messali M., Zarrok H., Errami M., Hammouti B., Bazzi Lh., Chakir A., *Der Pharm. Chem*. 4 (2012) 1496.
7. Ghazoui A., Bencaht N., Al-Deyab S.S., Zarrouk A., Hammouti B., Ramdani M., Guenbour M., *Int. J. Electrochem. Sci*. 8 (2013) 2272.
8. Zarrouk A., Zarrok H., Salghi R., Bouroumane N., Hammouti B., Al-Deyab S.S., Touzani R., *Int. J. Electrochem. S*ci. 7 (2012) 10215.
9. Bendaha H., Zarrouk A., Aouniti A., Hammouti B., El Kadiri S., Salghi R., Touzani R., *Phys. Chem. N*ews 64 (2012) 95.
10. Vasudevan T., Muralidharan S., Alwarappan S., S. Iyer V.K., *Corros Sci*. 37 (1995) 1235.
11. Muralidharan S.; Phani K. L. N., Pitchumani S., Ravichandran S., Iyer S. V. K., *J. Electrochem*. 142 (1995) 1483.
12. Benali O., Larabi L., Traisnel M., Gengembre L., Harek Y., *Appl. Surf. Sci*. 253 (2007) 6139.
13. Zarrouk A., Hammouti B., Zarrok H., Bouachrine M., Khaled K.F., Al-Deyab S.S., *Int. J. Electrochem. Sci*. 6 (2012) 89.
14. Ghazoui A., Saddik R., Benchat N., Guenbour M., Hammouti B., Al-Deyab S.S., Zarrouk A., *Int. J. Electrochem. Sci*. 7 (2012) 7080.
15. Zarrok H., Al Mamari K., Zarrouk A., Salghi R., Hammouti B., Al-Deyab S.S., Essassi E.M., Bentiss F., Oudda H., *Int. J. Electrochem. Sci*. 7 (2012) 10338.
16. Zarrok H., Zarrouk A., Salghi R., Ramli Y., Hammouti B., Assouag M., Essassi E.M., Oudda H., Taleb M., *J. Chem. Pharm. Res*. 4 (2012) 5048.
17. Popova A., Christov M., Zwetanova A, *Corros Sci*. 49 (2007) 2143.
18. Boudalia M., Bellaouchou A., Guenbour A., Bourazmi H., Tabiyaoui M., El Fal M., Ramli Y., Essassi El.M., Elmsellem H., *Mor. J. Chem*. 2 (2014) 97.
19. Zarrouk A., Hammouti B. , Dafali A. , Bentiss F. , *Ind. Eng. Chem. Res*. 52 (2013) 2560.
20. Zarrok H., Zarrouk A. , Salghi R., Oudda H. , Hammouti B. , Assouag M., Taleb M. , Ebn Touhami M., Bouachrine M. , Boukhris S. , *J. Chem. Pharm. Res*. 4 (2012) 5056.
21. Zarrok H., Oudda H., El Midaoui A., Zarrouk A., Hammouti B., Ebn Touhami M., Attayibat A., Radi S., Touzani R., *Res. Chem. Intermed*. 38 (2012) 2051.
22. ELouadi Y., Abrigach F.,Bouyanzer A., Touzani R.,Riant O., El Mahi B., El Assyry A.,Radi S., Zarrouk A.,Hammouti.B, *Der Pharma Chemica*, 7(2015) 265.
23. Ghazoui A., Zarrouk A., Bencaht N., Salghi R., Assouag M., El Hezzat M., Guenbour A., Hammouti B., *J. Chem. Pharm. Res*. 6 (2014) 704.
24. Zarrok H., Zarrouk A. , Salghi R. , Ebn Touhami M. , Oudda H. , Hammouti B., Touir R. , Bentiss F. , Al-Deyab S.S. , *Int. J. Electrochem. Sci*. 8 (2013) 6014.
25. Zarrouk A., Zarrok H., Salghi R., Touir R., Hammouti B., Benchat N., Afrine L.L., Hannache H., El Hezzat M., Bouachrine M., *J. Chem. Pharm. Res*. 5 (2013) 1482.
26. Belayachi M., Serrar H., El Assyry A., Oudda H., Boukhris H., Ebn Touhami M., Zarrouk A., Hammouti B., Eno Ebenso E., El Midaoui A., *Int. J. Electrochem. Sci*., 10 (2015) 3038.
27. Fouda A. S., Mousa M. N., Taha F. I., Elneamaa A. I., *Corros. Sci*. 26 (1986) 719.
28. Zarrok H., Zarrouk A., Salghi R., Assouag M., Hammouti B., Oudda H., Boukhris S., Al Deyab S.S., Warad I., *Der Pharm. Lett*. 5 (2013) 43.

29. Ben Hmamou D., Aouad M.R., Salghi R., Zarrouk A., Assouag M., Benali O., Messali M., Zarrok H., Hammouti B., *J. Chem. Pharm. Res*. 4 (2012) 3498.
30. Belayachi M., Serrar H., Zarrok H., El Assyry A., Zarrouk A., Oudda H., Boukhris S., Hammouti B., Ebenso Eno E., Geunbour A., *Int. J. Electrochem. Sci*. 10 (2015) 3010.
31. Tayebi H., Himmi B., Ramli Y., Zarrouk A., Geunbour A., Bellaouchou A., Zarrok H., Boudalia M., El Assyry M., *Res. J. Pharm., Biol. Chem. Sci.* 6 (2015) 1861.
32. Jafari H., Danaee I., Eskandari H., RashvandAvei M., *J. Environ. Sci. Health., Part A* 48 (2013) 1628.
33. Danaee I., Gholami M., RashvandAvei M., Maddahy M.H., *J. Ind. Eng. Chem*. 26 (2015) 81.
34. Ma, H., Chen, S., Liu, Z., Sun, Y., J. Mol. Struct., (THEOCHEM) 774 (2006) 19.
35. Henríquez-Román, J.H., Padilla-Campos, L., Páez, M.A., Zagal, J.H., María Rubio, A., Rangel, C.M., Costamagna, J., Cárdenas-Jirón, G., *J. Mol. Struct., (THEOCHEM)* 757 (2005) 1.
36. Rodrguez-Valdez, L.M., Martnez-Villafane, A., Glossman-Mitnik, D., *J. Mol. Struct. (THEOCHEM)* 713 (2005) 6.
37. Feng, Y., Chen, S., Guo, W., Zhang, Y., Liu, G., *J. Electroanal. Chem*., *602* (2007) 115.
38. Frisch, M.J., Trucks, G.W., Schlegel, H.B., Scuseria, G.E., Robb, M.A., Cheeseman, J.R., Montgomery, J.A.Jr., Vreven, T., Kudin, K.N., Burant, J.C., Millam, J.M., Iyengar, S.S., Tomasi, J., Barone, V., Mennucci, B., Cossi, M., Scalmani, G., Rega, N., Petersson, G.A., Nakatsuji, H.,Hada, M., Ehara, M., Toyota, K., Fukuda, R., Hasegawa, J., Ishida, M., Nakajima, T., Honda, Y., Kitao, O., Nakai, H., Klene, M., Li, X., Knox, J.E., Hratchian, H.P., Cross, J.B., Bakken, V., Adamo, C., Jaramillo, J., Gomperts, R., Stratmann, R.E., Yazyev, O., Austin, A.J., Cammi, R., Pomelli, C., Ochterski, J.W., Ayala, P.Y., Morokuma, K., Voth, G.A., Salvador, P., Dannenberg, J.J., Zakrzewski, V.G., Dapprich S., Daniels, A.D., Strain, M.C., Farkas, O., Malick, D.K., Rabuck, A.D., Raghavachari, K., Foresman, J.B., Ortiz, J.V., Cui, Q., Baboul, A.G., Clifford, S., Cioslowski, J., Stefanov, B.B., Liu, G., Liashenko, A., Piskorz, P., Komaromi, I.; Martin, R.L.; Fox, D.J.; Keith, T.; Al-Laham, M.A.; Peng, C.Y.; Nanayakkara, A.; Challacombe, M., Gill, P.M.W., Johnson, B., Chen, W., Wong, M.W., Gonzalez C., Pople, J.A., *Gaussian 03, Revision E.01, Gaussian, Inc., Wallingford CT*, 2004.
39. Solmaz R., Kardas G., Çulha M., Yazıcı B., Erbil M., *Electrochim Acta* 53 (2008) 5941.
40. Tao Z.H., Zhang S.T., Li W.H., Hou B.R., *Corros.Sci.* 51 (2009) 2588.
41. Ferreira E.S., Giacomelli C., Giacomelli F.C., Spinelli A., *Mater.Chem.Phys*. 83 (2004) 129. 42. Aljourani J., Raeissi K., Golozar M.A., *Corros. Sci*. 51 (2009) 1836.
43. Benali O., Larabi L., Traisnel M., Gengembra L., Harek Y., *Appl. Surf. Sci*. 253 (2007) 6130.
44. Quraishi M.A., Rawat J., *Mater. Chem. Phys*. 70 (2001) 95.
45. Amin M.A., El-Rehim S.S.A., El-Sherbini E.E.F., Bayoumy R.S., *Electrochim. Acta* 52 (2007) 3588.
46. Ehteram Noor A., Al-Moubaraki H., *Mater. Chem. Phys*. 110 (2008) 145.
47. Szauer T., Brandt A., *Electrochem. Acta* 26 (1981) 1219.
48. Guan N.M., Xueming L., Fei L., *Mater. Chem. Phys*. 86 (2004) 59.
49. Khamis E., Hosney A., El-Khodary S., *Afinidad* 52 (1995) 95.
50. Guan N.M., Xueming L., Fei L., *Mater. Chem. Phys*. 86 (2004) 59.
51. Kissi M., Bouklah M., Hammouti B., Benkaddour M., *Appl. Surf. Sci*. 252 (2006) 4190.
52. Machnikova E., Whitmire K.H., Hackerman N., *Electrochim. Acta*. 53(2008) 6024.
53. Olivares O., Likhanova N.V., Gomez B., Navarrete J., Llanos-Serrano M.E., Arce E., Hallen J.M., *Appl. Surf. Sci*. 252(2006) 2894.
54. Avci G., *Mater. Chem. Phys*. 112 (2008) 234.
55. Bayol E., Gurten A.A., Dursun M., Kayakırılmaz K., *Acta Phys. Chim. Sin*. 24 (2008) 2236.
56. Abiola O.K., Oforka N.C., *Mater. Chem. Phys*. 83 (2004) 315.
57. Ozcan M., Solmaz R., Kardas G., Dehri I., *Colloid Surf. A*. 325 (2008) 57.
58. Hongbo F., "Synthesis and application of new type inhibitors", Chemical Industry Press, Beijing, 2002, p.166.
59. Obot I.B., Obi-Egbedi N.O., *Corros. Sci*. 52 (2010) 657.
60. Jiajun F., Zang H., Wang Y., Li S., Chen T., Liu X., *Ind. Eng. Chem. Res.* 51 (2012) 6377.
61. Fu J., Li S., Wang Y., Liu X., Lu L., *J. Mater. Sci*. 46 (2011) 3550.
62. Obi-Egbedi N.O., Obot I.B., *Corros. Sci*. 53 (2011) 263.
63. Behpour M., Ghoreishi S.M., Khayatkashani M., Soltani N., *Corros. Sci*. 53 (2011) 2489.
64. Yadav D.K., Quraishi M.A., Maiti B., *Corros. Sci*. 55 (2012) 254.